Solitary Waves in the Critical Surface Tension Model

Yi A. Li
School of Mathematics
University of Minnesota
Minneapolis, MN   55455
yili@math.umn.edu

Brian Nguyen
Medtronic, Inc.
7000 Central Avenue N.E.
Minneapolis, MN   55432
brian.nguyen@medtronic.com

Peter J. Olver[†]
School of Mathematics
University of Minnesota
Minneapolis, MN   55455
olver@ima.umn.edu
http://www.math.umn.edu/∼olver

Abstract. This paper studies the properties of solitary wave solutions of a particular fifth order evolution equation that models water waves with surface tension. Existence and nonexistence results are surveyed and strengthened. An accurate numerical code is devised and used to show the small dispersive effects of solitary wave collisions.

1.   Introduction.

The importance of solitary waves in the study of nonlinear wave phenomena dates back to John Scott Russell's original experimental observations, [**35**], of waves generated in a canal; see [**34**] for historical details. Their existence remained controversial until Boussinesq, [**8**; eq. (30), p. 77], [**9**; eqs. (283, 291)], derived the unidirectional shallow water model

$$u_t + u_x + u u_x + u_{xxx} = 0, \tag{1}$$

now known as the Korteweg-deVries equation, and found the explicit sech^2 formula for its solitary wave solutions. In the 1960's, it was discovered that the the Korteweg-deVries

January 14, 1998

equation forms a completely integrable Hamiltonian system. Its solitary wave solutions are in fact solitons, meaning that they interact cleanly, [38, 15], having the same amplitude and velocity before and after collision, whose only effect is an overall phase shift. The alternative shallow water model

$$u_t + u_x + uu_x - u_{xxt} = 0, \tag{2}$$

proposed by Benjamin, Bona and Mahony, [7], also has explicit sech[2] solitary wave solutions, but is not integrable, and one numerically observes small dispersive effects when the waves collide, [1].

Both shallow water models (1) and (2) are first order in the Boussinesq perturbation expansion and serve to model weak nonlinearities. Fully nonlinear models have been recently shown to admit non-analytic solitary wave solutions, [11, 33]. Quite a number of higher order weakly nonlinear models, including three integrable cases: the fifth order Korteweg–deVries, Sawada–Kotera, and Kaup equations. We refer the reader to [27] for a comprehensive survey of the different models and their solitary wave solutions. Such higher order equations exhibit a variety of solitary wave phenomena, ranging from exact soliton solutions, to nonintegrable cases which admit exact sech[2] solutions, to models (which include most of those of relevance in shallow water theory) that do not admit solitary wave solutions at all.

In this work, we concentrate on the simplest and most well studied case. The fifth order nonlinear evolution equation

$$u_t + (u^2)_x + u_{xxx} + \varepsilon u_{xxxxx} = 0 \tag{3}$$

is known as the *critical surface tension model*. This equation arises in the modeling weakly nonlinear waves in a wide variety of media, including magneto-acoustic waves in plasmas, [24], long waves in liquids under ice sheets, [21, 30], and water waves with surface tension when the Bond number is near the critical value $\tau = \frac{1}{3}$, which is the one situation where the usual Korteweg–deVries model (1) no longer applies, cf. [2, 18, 25].

The existence and nature of solitary wave solutions for (3) is dependent on the sign of the parameter ε multiplying the fifth order term. When $\varepsilon > 0$, a dynamical systems argument, [2, 17], shows that (3) admits traveling wave solutions that decay to zero at $x \to +\infty$. However, Amick and McLeod, [2], and Eckhaus, [13, 14], rigorously proved that the model (3) does not possess a solitary wave of elevation for $\varepsilon > 0$ sufficiently small. In this paper, we extend their result to all positive ε. On the other hand, Kichenassamy, [26], uses a variational approach to prove the existence of "dark" solitary waves, meaning waves of depression that have negative wave speeds.

For the model (3) with $\varepsilon < 0$, Yamamoto and Takizawa, [37], produced an explicit solitary wave solution at one particular (positive) wave speed in terms of a sech[4] function:

$$u(x,t) = -\frac{105}{338\varepsilon} \operatorname{sech}^4\left[\sqrt{\frac{-1}{52\varepsilon}}\left\{x + \frac{36}{169\varepsilon}t\right\}\right]. \tag{4}$$

Proof of existence of such solitary wave solutions for a range of wave speeds, which includes the known exact solution, can be found in [3, 12, 20], and their nonlinear stability is proved

in [22]. In recent numerical studies of the break-up of initial data, Hyman and Rosenau, [19] have observed a variety of localized pulsating "multiplet" solutions.

More general types of "semi-localized" solitary wave solutions have also been investigated. Kawahara, [25], gave the first numerical evidence of oscillatory solitary wave solutions, which no longer decay to zero, but have small amplitude oscillatory tails at large distances. These solutions are rigorously characterized as singular perturbations of Korteweg–deVries solitons, [31, 18, 20]. In addition, envelope solitary wave solutions were discovered in [16]. Numerical experiments on semi-localized solutions and their interactions appear in [10, 5, 29].

In this paper, we present a general proof of the nonexistence of solitary wave solutions traveling to the right (respectively left) when $\varepsilon > 0$ (respectively $\varepsilon < 0$). We then discuss some of our preliminary numerical computations of the collisions between two localized solitary waves, showing that dispersive effects are present, albeit of extremely small amplitude. A highly accurate numerical scheme is required to unambiguously detect the dispersive remnants of a collision. These results form part of an ongoing study of the solitary wave solutions of the general class of higher order nonlinear evolution equations.

2. Nonexistence of Solitary Waves.

In this section, we shall prove that the fifth order evolution equation (3) has no solitary wave solutions traveling to the right when $\varepsilon > 0$, and has no solitary wave solutions traveling to the left when $\varepsilon < 0$. The elementary rescaling

$$u(x,t) \longmapsto -\sqrt[5]{\varepsilon}\, u\left(-\frac{x}{\sqrt[5]{\varepsilon}}, t\right)$$

reduces (3) to

$$u_t + (u^2)_x + \mu u_{xxx} - u_{xxxxx} = 0, \tag{5}$$

with $\mu = -\varepsilon^{-3/5}$. (The minus sign has been chosen so that the solitary wave solutions that do exist are waves of elevation traveling to the right.) To prove the nonexistence result, it suffices to show that the equation (5) has no solitary wave solutions traveling to the left for any constant $\mu \in \mathbb{R}$.

The equation for traveling waves is obtained by substituting the ansatz $u = \phi(x - c\,t)$, where c is the wave speed, into the equation (5):

$$-c\phi' + 2\phi\phi' + \mu\phi''' - \phi^{(5)} = 0.$$

Integrating once and, for $c < 0$, rescaling via $\phi(x) = c\,\varphi(\sqrt[4]{-c}\,x)$, we obtain

$$-\varphi + \varphi^2 + p\varphi'' + \varphi^{(4)} = 0, \tag{6}$$

where $p = -(-c)^{-1/2}\mu$. The integration constant was set to zero since we are interested in existence of solitary wave solutions that decay to zero at infinity. Equation (6) is a four-dimensional dynamical system having a fixed point at the origin $(0,0,0,0)$ near which there are a two-dimensional center manifold, a one-dimensional stable manifold and a one-dimensional unstable manifold. A solitary wave solution will exist if and only if the stable and unstable manifolds intersect.

3

Lemma 1. *Any orbit in the stable manifold at the origin of* (6) *has a Dirichlet expansion of the form*

$$\varphi(x) = \sum_{n=1}^{\infty} c_n e^{-\lambda n x}, \qquad \text{where} \qquad \lambda = \sqrt{\frac{-p + \sqrt{p^2 + 4}}{2}} \,. \tag{7}$$

The series (7) *is convergent on the interval* (x_0, ∞) *and has an analytic extension to the half plane* $\{z \in \mathbb{C} \mid Re\, z > x_0\}$, *where* $x_0 > -\infty$ *is the abscissa of convergence of* (7).

Proof: The fact that any orbit in the stable manifold has an expansion of the form (7) for x sufficiently large is a particular case of the result in [**27**; Theorem 7], which applies to more general fifth order models; see also [**28**]. The coefficients c_n satisfy the recursion relation

$$c_n = \frac{-1}{\lambda^4 n^4 + p\lambda^2 n^2 - 1} \sum_{k=1}^{n-1} c_{n-k} c_k = \frac{-1}{(\lambda^4 n^2 + 1)(n^2 - 1)} \sum_{k=1}^{n-1} c_{n-k} c_k, \qquad n \geq 2, \tag{8}$$

which follows immediately upon substituting (7) into (6). Note that $c_n = c_1^n d_n$, where d_n satisfies the same recurrence (8) with $d_1 = 1$. A simple inductive argument shows that $\{d_n\}$ is an alternating sequence with $|d_n| < 2^{1-n}$, which implies that (7) converges for $x > \lambda^{-1} \log \frac{1}{2} |c_1|$. Let x_0 denote the infimum of the set of all x's for which (7) converges. We claim that $x_0 > -\infty$. Note that

$$J_n = \frac{1}{\left(\lambda^4 + \frac{1}{n^2}\right)\left(1 - \frac{1}{n^2}\right)} \sum_{k=1}^{n-1} \left(1 - \frac{k}{n}\right)^4 \left(\frac{k}{n}\right)^4 \frac{1}{n} \longrightarrow \frac{B(5,5)}{\lambda^4} \qquad \text{as} \qquad n \longrightarrow \infty,$$

where $B(\alpha, \beta)$ is the usual Beta function. Choose $N > 0$ so that $J_n > \frac{1}{n}$ whenever $n \geq N$. We shall prove by induction that

$$|d_n| \geq a^n n^4, \qquad \text{where} \qquad a = \min \left\{ \sqrt[k]{\frac{|d_k|}{k^4}} \; \middle| \; 1 \leq k \leq N \right\}. \tag{9}$$

The required estimate holds for $1 \leq k \leq N$ by the definition of a. To prove the induction step, let $n \geq N$; then

$$|d_{n+1}| = \frac{\sum_{k=1}^{n} |d_{n+1-k} d_k|}{(\lambda^4 (n+1)^2 + 1)((n+1)^2 - 1)}$$

$$\geq \frac{a^{n+1} \sum_{k=1}^{n} (n+1-k)^4 k^4}{(\lambda^4 (n+1)^2 + 1)((n+1)^2 - 1)} = a^{n+1}(n+1)^5 J_{n+1} \geq a^{n+1}(n+1)^4.$$

As a result of (9), the abscissa of convergence of (7) satisfies $x_0 \geq \lambda^{-1} \log a |c_1|$.   *Q.E.D.*

It follows from Lemma 1 that in the $\varphi \varphi' \varphi'' \varphi'''$-phase space, there are only two orbits approaching the fixed point $(0,0,0,0)$. One orbit corresponds to the series expansion (7) with the coefficient $c_1 > 0$, going to the origin in the direction $(-1, \lambda, -\lambda^2, \lambda^3)$. The other orbit has the series expansion (7) with the coefficient $c_1 < 0$, approaching the origin from the direction opposite to $(-1, \lambda, -\lambda^2, \lambda^3)$. The latter orbit is not a homoclinic orbit because its Dirichlet expansion has a singularity at its abscissa of convergence.

Lemma 2. *If $c_1 < 0$, then the sum φ of the Dirichlet expansion (7) has a singularity at its abscissa of convergence x_0; in fact $\lim_{x \to x_0^+} \varphi(x) = -\infty$.*

Proof: If $c_1 < 0$, then $c_n = c_1^n d_n < 0$ for all n, which implies that φ has a singularity at its abscissa of convergence, cf. [**36**]. Assume that $\inf_{x > x_0} \varphi(x) > -\infty$. Since $\varphi'(x) > 0$ and $\varphi(x) < 0$, φ is an increasing function with a lower bound on the interval (x_0, ∞). Therefore, the limit $\lim_{x \to x_0^+} \varphi(x) = m < 0$ exists. When $x > x_0$, the derivatives of φ can be expressed by, [**2**],

$$\varphi^{(j)}(x) = \frac{1}{p} \int_x^\infty K(x - y) \frac{d^{j-1}}{dy^{j-1}} \left(\varphi(y)^2 - \varphi(y) \right) dy, \tag{10}$$

where

$$K(z) = \begin{cases} 1 - \cos \sqrt{p}\, z, & p > 0, \\ \cosh \sqrt{-p}\, z - 1, & p < 0. \end{cases}$$

If $\varphi(x_0)$ exists, then (10) allows us to also continuously define $\varphi^{(j)}(x_0)$. But, given the initial conditions $\varphi(x_0), \varphi'(x_0), \varphi''(x_0), \varphi'''(x_0)$, the classical theory of ordinary differential equations shows that the solution φ to (6) has an analytic extension in a neighborhood of x_0, which contradicts the fact that φ has a singularity there.   *Q.E.D.*

The remaining question is whether the solution represented by (7) with $c_1 > 0$ is a homoclinic orbit. We shall use the following result to discuss this issue.

Theorem 3. *For any $p \in \mathbb{R}$, there exists a unique solution of the boundary value problem*

$$-\varphi + \varphi^2 + p\varphi'' + \varphi^{(4)} = 0, \qquad \varphi'(0) = \varphi(\infty) = 0. \tag{11}$$

The solution satisfies $\varphi'(x) < 0$ for $x > 0$, and $\varphi'''(0) > 0$.

Proofs of Theorem 3 in the case $p > 0$ can be found in [**2, 17**]. The case $p \leq 0$ is proved similarly, so we shall omit the full argument here. We next prove the symmetry of solitary wave solutions; see [**6**] for the corresponding result for waves with oscillatory tails.

Lemma 4. *A solitary wave solution of (6) is symmetric with respect to some point x_1, so $\varphi(x_1 + x) = \varphi(x_1 - x)$ for all x.*

Proof: Equation (6) is invariant under reflection $x \mapsto -x$. As a consequence, if $\varphi(x)$ is an orbit in the unstable manifold, then $\varphi(-x)$ is an orbit in the stable manifold, and so has a Dirichlet expansion

$$\varphi(x) = \sum_{n=1}^\infty a_1^n d_n e^{\lambda n x}, \tag{12}$$

where $a_1 > 0$, for x sufficiently large negative. Comparing the two series (7), (12), we infer that $x_1 = \frac{1}{2\lambda} \log \frac{c_1}{a_1}$ should be the point of symmetry. Indeed, $\varphi(2x_1 + x)$ and $\varphi(-x)$ have the same convergent Dirichlet series for x sufficiently large, and so the analyticity of solitary wave solutions, as indicated by (10), and the classical theory of ODE, [**23**; p. 281], imply that they are equal: $\varphi(2x_1 + x) = \varphi(-x)$ for all $x \in \mathbb{R}$.   *Q.E.D.*

If the function φ in Theorem 3 is a solitary wave solution, then 0 cannot be its point of symmetry, which must therefore be negative, since $\varphi''(0) \neq 0$. We shall use this observation combined with Theorem 3 to show nonexistence of solitary wave solutions, thereby generalizing the results in [**2**].

Theorem 5. *For any constant p, the dynamical system* (6) *has no homoclinic orbit near the origin, i.e., there is no bounded solution φ of* (6) *that satisfies*

$$\lim_{x \to \infty} \varphi(x) = 0 = \lim_{x \to -\infty} \varphi(x).$$

Proof: Assume that (6) has a solitary wave solution φ. Since (6) is translation invariant, one may let its point of symmetry be $x_1 = 0$, and so φ is an even function. Theorem 3 implies that there is a point $x_0 > 0$ such that

$$\begin{aligned}
\varphi'(x_0) = \varphi'(-x_0) = 0, &\qquad \varphi'''(x_0) = -\varphi'''(-x_0) > 0, \\
\varphi(x_0) = \varphi(-x_0) > \tfrac{3}{2}, &\qquad \varphi''(x_0) = \varphi''(-x_0) < 0.
\end{aligned} \tag{13}$$

The inequality $\varphi(x_0) > \frac{3}{2}$ follows from the useful identity

$$\varphi'\varphi''' = -\frac{p(\varphi')^2}{2} + \frac{\varphi^2}{3}\left(\frac{3}{2} - \varphi\right) + \frac{(\varphi'')^2}{2}, \tag{14}$$

which results from multiplying (6) by φ' and integrating once.

Let us first assume $p \leq 0$. Then $-p\varphi''(-x_0) \leq 0$ and $\varphi(-x_0)(1 - \varphi(-x_0)) < 0$, so that the equation (6) implies that $\varphi^{(4)}(-x_0) < 0$. As long as $\varphi^{(4)}(x)$ remains negative, for $x > -x_0$, $\varphi, \varphi', \varphi'', \varphi'''$ will all be decreasing functions, with $\varphi', \varphi'', \varphi'''$ remaining strictly negative. However, since φ is an even function, it has to stop decreasing at some point in the interval $(-x_0, 0]$. Therefore, there is a point $-x_0 < x_1 < 0$ such that $\varphi^{(4)}(x_1) = 0$. Since $\varphi'(x_1), \varphi''(x_1), \varphi'''(x_1) < 0$, equation (6) implies that $0 \leq \varphi(x_1) \leq 1$. For $x > x_1$, $\varphi, \varphi', \varphi''$ will continue to decrease as long as $\varphi''' < 0$. Suppose $x_2 > x_1$ is the first point where $\varphi'''(x_2) = 0$. Since $\varphi''(x_2) < 0$ and $\varphi(x_2) < 1$, the right-hand side of (14) is positive, which is a contradiction, and hence φ''' cannot vanish for $x > x_1$, which means that φ will decrease for all $x > x_1$. However, this contradicts the original assumption that φ is an even function, and hence homoclinic orbits do not exist when $p \leq 0$.

In fact, we can show that φ blows up at some finite point. Assume that φ is defined on the real line. It follows from the above proof that φ is increasing, $\varphi'(x) > 0$ and $\varphi''(x) < 0$ when $x < x_0$. This implies that $\varphi(x) \to -\infty$ as $x \to -\infty$, and hence there exists a point x_3 where $\varphi(x_3) = 0$ and $\varphi(x) < 0$ for $x < x_3$. Multiplying both sides of (14) by φ' and integrating from x to x_3, one obtains

$$\begin{aligned}
\varphi'(x)^2 \varphi''(x) &= \frac{\varphi(x)^3}{6} - \frac{\varphi(x)^4}{12} + \varphi'(x_3)^2 \varphi''(x_3) - \int_x^{x_3}\left(-\frac{p}{2}\varphi'(y)^3 + \frac{5}{2}\varphi'(y)\varphi''(y)^2\right)dy \\
&\leq \frac{\varphi(x)^3}{6} - \frac{\varphi(x)^4}{12}.
\end{aligned}$$

Multiplying both sides of the latter inequality by φ' and integrating again leads to

$$\varphi'(x)^4 \geq \left(\varphi'(x_3)\right)^4 + \frac{\varphi(x)^4}{6} - \frac{\varphi(x)^5}{15} \geq -\frac{\varphi(x)^5}{15}\,.$$

We conclude that

$$\varphi(x) \le \frac{\varphi(y)}{\left(1 - \frac{1}{4}(y - x) \sqrt[4]{-\frac{1}{15}\varphi(y)} \ \right)^4}$$

for $x < y < x_3$ sufficiently close to x_3, and hence φ must blow up at some finite point.

Now suppose that $p > 0$. Again, assume that (6) has an even solitary wave solution φ, satisfying conditions in (13). Integrating (6) on the interval $(-x_0, x)$ yields

$$\varphi'''(x) + p\varphi'(x) = \int_{-x_0}^{x} \left[\varphi(y) - \varphi(y)^2 \right] dy + \varphi'''(-x_0). \tag{15}$$

If $\varphi(x) \ge 1$ for $-x_0 < x < x_0$, then (15) implies $\varphi'''(x) + p\varphi'(x) \le 0$, which contradicts the fact that $\varphi'''(x_0) + p\varphi'(x_0) > 0$. Hence, there must be a point $\tilde{x} \in (-x_0, x_0)$ such that $\varphi(\tilde{x}) < 1$. Let $-x_0 < x_1 < x_0$ be the first point after x_0 where $\varphi(x_1) = \frac{3}{2}$. Then $\varphi'(x_1) \le 0$; moreover, if $\varphi'(x_1) = 0$, then (14), (15) imply that $\varphi''(x_1) = 0$, $\varphi'''(x_1) < 0$. Therefore, $\varphi'(x) < 0$ for nearby $x > x_1$. Moreover, once $\varphi(x) < \frac{3}{2}$, the derivative $\varphi'(x)$ must remain negative except for possibly one point. Suppose that $x_2 > x_1$ is the first point satisfying $\varphi'(x_2) = 0$. Since $\varphi(x_2) < \frac{3}{2}$, it follows from (14) that $\varphi(x_2) = \varphi''(x_2) = 0$, and $\varphi'''(x_2) \ne 0$ as otherwise φ would be a trivial solution. In fact, $\varphi'''(x_2) < 0$ because if it were positive, we would have $\varphi'(x) > 0$, $\varphi(x) < 0$, for nearby $x < x_2$. Thus, $\varphi'(x) < 0$, $\varphi(x) < 0$ when $x > x_2$. Equation (14) implies that that φ' will remain negative for all $x > x_2$, so φ is decreasing, which contradicts our original assumption that φ is a homoclinic orbit represented by an even function. We conclude that (6) has no solitary wave solutions when $p > 0$ also.

The last issue to discuss is how $\varphi(x)$ behaves for $x < x_0$. Let

$$k(x) = \frac{1}{p} \left[x - \frac{\sin(\sqrt{p}\,x)}{\sqrt{p}} \right]. \tag{16}$$

Note that $k(x) < 0$ for $x < 0$, while $0 \le k'(x) \le 1/p$, $-1 \le k'''(x) \le 1$ for all x. Then

$$\varphi(x) = -\int_{x}^{x_0} k(x - y)\big(\varphi(y) - \varphi(y)^2\big)\, dy + p\,\varphi(x_0)k'(x - x_0) +$$
$$+ \sum_{j=0}^{3} \varphi^{(j)}(x_0)k^{(3-j)}(x - x_0), \tag{17}$$

In view of (13), this implies that

$$\varphi(x) \le \varphi(x_0)k'''(x - x_0) + p\,\varphi(x_0)k'(x - x_0), \tag{18}$$

provided $\varphi(y) \ge 1$ for all $y \in [x, x_0]$. The left hand-side of (18) is bounded and thus $\varphi(x) \le 3\varphi(x_0)$. On the other hand,

$$\varphi''(x) + p\varphi(x) = -\int_{x}^{x_0} (x - y)\big(\varphi(y) - \varphi(y)^2\big)\, dy$$
$$+ \varphi''(x_0) + p\varphi(x_0) + \varphi'''(x_0)(x - x_0). \tag{19}$$

7

If $\varphi(x) \geq 1$ for all $x < x_0$, then $\varphi''(x) + p\varphi(x) \leq p\varphi(x_0) + \varphi'''(x_0)(x - x_0) \to -\infty$ as $x \to -\infty$, which is impossible. On the other hand, once $\varphi(x) < 1$, its derivative φ' remains non-negative, so $\varphi(x)$ decreases as x decreases. Suppose that φ is defined everywhere and $\lim\limits_{x \to -\infty} \varphi(x) = c_0$ exists. If $c_0 > 0$, then the identity

$$\varphi'''(x) + p\varphi'(x) = \int_x^{x_0} \left[\varphi(y)^2 - \varphi(y) \right] dy + \varphi'''(x_0) \tag{20}$$

would imply that $\varphi(x) \to \infty$ as $x \to -\infty$. If $c_0 < 0$, then (19) would imply that $\varphi(x) \to -\infty$ as $x \to -\infty$. Thus, $c_0 = 0$. Since $\varphi'(x) \geq 0$ for all x sufficiently large negative, (20) implies that $\int_{-\infty}^{x_0} \left(\varphi(y)^2 - \varphi(y) \right) dy$ converges, and hence, $\lim\limits_{x \to -\infty} [\varphi'''(x) + p\varphi'(x)] = c_1$ exists. Integrating, we deduce that $c_1 = 0$ is necessary for φ to remain bounded. Since $\varphi(x) - \varphi(x)^2 > 0$ for all $-x$ sufficiently large, (10) implies that φ' is bounded, which shows that $\varphi'(x)$, $\varphi''(x)$ and $\varphi'''(x) \to 0$ as $x \to -\infty$. Therefore, φ is a homoclinic orbit of the system (6). But we already know that (6) has no homoclinic orbits, and hence the solution φ is not bounded below. As a matter of fact, φ also blows up at a finite point, which may be shown by using an argument similar to that in [**2**]. $\hfill Q.E.D.$

3. Numerical Analysis.

Solitary-wave solutions $u(x,t) = \phi(x - ct)$ of the critical surface tension model (5) exhibit an interesting property that for each speed $\mu \geq 2\sqrt{c} > 0$ there is an even, monotone localized solitary wave solution, while if $2\sqrt{c} > |\mu|$, the solitary waves become oscillatory at $\pm\infty$. For the numerical simulation of collisions between localized solitary waves, we choose $\mu = 13/6$ and two non-oscillatory solitary waves. One has the closed form (4), so under the rescaling indicated above,

$$u(x,t) = \frac{35}{24} \operatorname{sech}^4 \frac{x - t}{2\sqrt{6}}.$$

A second solitary wave solution was obtained using a numerical approximation based on the results of Amick and Toland, [**3**]. The non-oscillatory solitary waves are represented by even functions satisfying the initial conditions

$$\phi'(0) = \phi'''(0) = 0, \qquad\qquad\qquad \phi''(0) < 0,$$
$$c - \tfrac{1}{12} \left[\mu^2 + \mu\sqrt{\mu^2 + 12c} \right] < \phi(0) < \tfrac{3}{2} c, \qquad \phi''(0)^2 - c\phi(0)^2 + \tfrac{2}{3}\phi(0)^3 = 0.$$

For the wave speed $c = (13/18)^2 = 0.521605$, we used a standard Runge-Kutta method to numerically solve the initial value problem, and an interactive procedure to determine the initial data leading to a solution $\phi(x)$ that is monotonically decreasing to zero as $x \to \infty$. The resulting initial conditions are

$$\phi(0) = 0.76807209085436767, \quad \phi''(0) = -0.0750861780309212, \quad \phi'(0) = \phi'''(0) = 0.$$

The solution $\phi(x)$ is used as a numerical estimation of the second solitary wave solution.

The remainder of this section describes the experiment to simulate two solitary wave solutions of the critical surface tension model and their collision. The numerical simulations are performed using conservative, sixth-order accurate finite-differences in space and

8

the trapezoid method for stepping in time. The trapezoid method is chosen for its stability characteristics. The Fourier footprint of the central differences in space lies on the imaginary axis, for which the trapezoid method is neutrally stable, independent of the temporal step size. Methods with higher formal order of accuracy than the trapezoid method, such as the Runge-Kutta method, may be used, although their conditional stability requires an exponentially small time step. Other methods have positive damping, which may affect the small dispersive waves over long integration times, making it difficult to differentiate dispersive effects from plain numerical errors.

Periodic boundary conditions are used for the computations. These boundary conditions were chosen to avoid the introduction of spurious reflections due to the imperfections of "non-reflecting" boundary conditions.

The finite difference approximations used are determined uniquely by writing the Taylor series expansion of the solution at each point on the grid, and combining the expansions of nearby points to cancel out unwanted terms. The results are

$$(u^2)_x = \frac{-(u^2)_{i-3} + 9(u^2)_{i-2} - 45(u^2)_{i-1} + 45(u^2)_{i+1} - 9(u^2)_{i+2} + (u^2)_{i-3}}{60h} + O(h^6),$$

$$u_{xxx} = \frac{\left[\begin{array}{c} -7u_{i-4} + 72u_{i-3} - 338u_{i-2} + 488u_{i-1} - \\ -488u_{i+1} + 338u_{1+2} - 72u_{i+3} + 7u_{i+4} \end{array}\right]}{240h^3} + O(h^6), \qquad (21)$$

$$u_{xxxxx} = \frac{\left[\begin{array}{c} -13u_{i-5} + 152u_{i-4} - 783u_{i-3} + 1872u_{i-2} - 1938u_{i-1} + \\ +1938u_{i+1} - 1872u_{i+2} + 783u_{i+3} - 152u_{i+4} + 13u_{i+5} \end{array}\right]}{288h^5} + O(h^6),$$

where h is the uniform grid spacing. Let $\mathbf{U}$ be the vector of discretized solutions. The resulting semi-discrete equation has the form

$$\mathbf{U}_t + \mathbf{F}(\mathbf{U}) = 0,$$

where $\mathbf{F}(\mathbf{U})$ is the finite difference approximation for the spatial derivatives based on (21). Using the trapezoid method, one writes

$$\frac{(\Delta \mathbf{U})^n}{\Delta t} + \frac{\mathbf{F}(\mathbf{U}^n) + \mathbf{F}(\mathbf{U}^{n+1})}{2} = 0,$$

where $(\Delta \mathbf{U})^n = \mathbf{U}^{n+1} - \mathbf{U}^n$. The term $\mathbf{F}(\mathbf{U}^{n+1})$ cannot be computed at time step n. Therefore, we use the method of replacing it with its Taylor expansion, [4],

$$\mathbf{F}(\mathbf{U}^{n+1}) = \mathbf{F}(\mathbf{U}^n) + \mathbf{A}(\mathbf{U})(\Delta \mathbf{U})^n + \cdots,$$

where $\mathbf{A}(\mathbf{U})$ is the Jacobian matrix $\partial \mathbf{F}(\mathbf{U})/\partial \mathbf{U}$. Note that $\mathbf{A}(\mathbf{U})$ is not constant, because $\mathbf{F}(\mathbf{U})$ is non-linear. We replace ulA by its average between adjacent time steps, resulting in the equation

$$\frac{(\Delta \mathbf{U})^n}{\Delta t} + \mathbf{F}(\mathbf{U}^n) + \frac{1}{2}\left[\mathbf{A}(\mathbf{U}^n) + \mathbf{A}(\mathbf{U}^{n+1})\right](\Delta \mathbf{U})^n = 0. \qquad (22)$$

A linear equation solver cannot be applied to this equation due to the $\mathbf{U}^{n+1}$ term. However, the iterative method

$$\frac{(\Delta \mathbf{U})^{n,k+1}}{\Delta t} + \mathbf{F}(\mathbf{U}^n) + \frac{1}{2}\left[\mathbf{A}(\mathbf{U}^n) + \mathbf{A}(\mathbf{U}^n + (\Delta \mathbf{U})^{n,k})\right](\Delta \mathbf{U})^{n,k+1} = 0,$$
$$(\Delta \mathbf{U})^{n,0} = 0,$$
(23)

may be used until $\|(\Delta \mathbf{U})^{n,k+1} - (\Delta \mathbf{U})^{n,k}\| < \delta$, at which point $(\Delta \mathbf{U})^n = (\Delta \mathbf{U})^{n,k+1}$ solves (22) and gives $\mathbf{U}^{n+1}$. In this work, we use $\delta = 10^{-14}$. The linear system solver uses a direct banded-diagonal solver with partial pivoting. The Woodbury formula, [**32**], is used to modify the resulting solution for the effects of the out-of-band terms (caused by the periodic boundary conditions). After the direct solve, iterative improvements, [**32**], are applied until the L^2 norm of the error of the final linear algebra solution is less than 10^{-12}.

The numerical algorithm is validated on equation (5) using the exact solitary wave solution for comparison. The error

$$\left\|\sum_i \left\{\mathbf{U}^n(x_i) - u(x_i, t^n)\right\}\right\|$$

grows linearly from zero at $t = 0$ to 1.8×10^{-5} at $t = 1600$, which is deemed to be sufficiently low. (The simulation is performed without the dispersion damping mechanism described below.) The simulations are carried out with grid spacings of $h = \frac{1}{8}$ and time steps of $\Delta t \approx 0.00215$ for the exact solution and $\Delta t \approx 0.00406$ for the second solution. For the collision, the smaller time step size is used.

In propagating the second solitary wave solution, it is found that the initial (ODE) solution described above was insufficiently close to a solitary wave, in that small, but significant, dispersion does take place. Before experimenting on solitary wave collisions, a second clean solitary wave is required. This can be done by giving the dispersive waves sufficient time to leave the proximity of the primary wave structure. In order to avoid the excessively large computational domain occupied by the quickly dispersing waves, a method of selectively damping waves in the domain is employed. First, the primary wave structure is kept at the center of the grid by moving the grid along with it. After each time step, if the grid point corresponding to the maximum U is not the middle grid point, the grid is shifted in integer grid spacings so that the middle grid point does coincide with the maximum U. Periodicity of the solution is used in determining the solution of the points that has entered the computational domain due to the grid shifting. Note that this procedure does not alter the numerical method in any way. Second, while keeping the primary wave structure at the center of the grid, exponential damping is applied to the outer quarters of the grid. This takes the form of changing the solution obtained from (22) by

$$U_i^{n+1} \longleftarrow U_i^{n+1} e^{-\sigma \gamma(x_i)\Delta t}$$

The function $\gamma(x)$ is chosen so that it is zero in the middle half of the grid, grows smoothly in the outer quarters of the grid and reaches 1 at the boundaries of the grid. The parameter σ is used to control the level of damping. It is set to $\frac{1}{2}$ during damping and to zero to turn off damping. For a 2048-interval grid, the function $\gamma(x)$ is shown in Figure 6.

10

Each time damping is performed, the L^2 norm of the difference between the solutions before and after damping, i.e.,

$$\frac{1}{\Delta t} \frac{\sum_i (U_i - U_i^*)^2}{\sum_i (U_i^*)^2} \, ,$$

is computed and normalized as shown. The variable U^* is that given by the finite difference scheme, before the damping step is applied. They are plotted in Figure 5 for the exact wave solution and the second wave solution. To ensure that dispersive wave damping does not affect the non-dispersive part of the wave, it is turned off at $t = 800$, after dispersion has stopped. The wave is further propagated to $t = 1600$ without damping to ensure that it has stopped dispersing. At that time, no significant signals are seen outside the primary wave structure, indicating that the wave is no longer dispersive. The figures below will show that the solution in the regions away from the primary wave structure remain acceptably near zero.

After obtaining the two solitary wave solutions at $t = 1600$, their speeds and shapes are studied to further check for the appropriate behavior, i.e., that they remain constant as the waves evolve. Each wave is propagated a little further, while at each time step, a cubic spline fit is made for the solution, over the entire domain. The peak is estimated as the global maximum of the spline, thus it may occur between grid points. The change in peak location is divided by time step size to obtain the peak speed. The speeds at each time step as well as the average speed since $t = 1600$ are shown in Figures 1 and 2. In addition to checking wave speed, we check the wave shape by computing the L^2 norm of the difference between each solution after $t = 1600$ and the solution at $t = 1600$. This difference is shown in Figures 3 and 4 for the two waves. They are quite small and do not appear to be increasing. The oscillatory behavior of Figures 1 through 4 are due to the cycle of wave peak as it passes through each grid interval, reflecting the variation in the cubic spline fit.

For the collision experiment, the two solutions associated with the curves in Figure 5 are used. The independently simulated solutions are combined in one grid for the collision experiment. The solutions are shifted so that the faster wave is behind the slower wave. After assembly, the waves are propagated for another 1024 time units. After 512 time units (still before the waves collide) the solution is shown in Figure 7. Note in this figure and those following that the boundary condition is periodic, the grid continues to be shifted to be centered around the highest point in the solution and no damping is applied. The range $[-.004, .004]$ on the abscissa is called the dispersion scale (in anticipation of the post-collision dispersion). Figure 8 shows that before the collision, no dispersion exists. The disturbances of these solutions are visible only at the error scale of $[-10^{-9}, 10^{-9}]$, as shown in Figure 9. In interpreting the collision results, any disturbances greater than the error scale will be considered dispersion.

After the collision, the solution is shown in full scale in Figure 10. Dispersion is not visible on this scale. However Figure 11 shows disturbances that are five orders of magnitude larger than the error scale, trailing the two primary wave structures. By comparison to the expected errors, this is considered to be dispersion rather than numerical errors. Therefore, we conclude that the dispersion amplitude is approximately .06% of the maximal wave height. This compares with a dispersive effect of about .3% that has

11

been observed in the BBM model (2) in [**1**], indicating that the solitary wave solutions of the critical surface tension model can be considered as an order of magnitude closer to "integrable" than their BBM counterparts.

4. Conclusions.

In conclusion, we have demonstrated that in certain regimes, there are no solitary wave solutions for the critical surface tension model. In the regimes where such solutions exist, they can be accurately approximated using finite difference numerical algorithms. As expected, upon collision they experience a small dispersive effect, which indicates the non-integrability of the model. What is surprising is how small this dispersive interaction is, which indicates that the model is, in some sense, extremely close to integrable, even though the "nearest" known integrable fifth order models are not particularly close in any known analytical sense. The numerical studies of these solutions will be continued, and we hope to report on the results of break up of initial data, multiple collision effects, and extensions to multiplet, oscillatory and envelope solitary waves in a subsequent publication.

References

[**1**] Abdulloev, K.O., Bogolubsky, I.L., and Makhankov, V.G., One more example of inelastic soliton interaction, *Phys. Lett. A* **56** (1976), 427–428.

[**2**] Amick, C.J., and McLeod, J.B., A singular perturbation problem in water waves, *Stability Appl. Anal. Contin. Media* **1** (1991), 127–148.

[**3**] Amick, C.J., and Toland, J.F., Homoclinic orbits in the dynamic phase-space analogy of an elastic strut, *European J. Appl. Math.* **3** (1992), 97–114.

[**4**] Ashford, G., *An Unstructured Grid Generation and Adaptive Solution Technique for High-Reynolds-Number Compressible Flows*, Ph.D. Thesis, University of Michigan 1996.

[**5**] Bakholdin, I., and Il'ichev, A., Radiation and modulational instability described by the fifth-order Korteweg–deVries equation, *Contemp. Math.* **200** (1996), 1–15.

[**6**] Benilov, E.S., Grimshaw, R., and Kuznetsova, E.P., The generation of radiating waves in a singularly-perturbed Korteweg–deVries equation, *Physica D* **69** (1993), 270–278.

[**7**] Benjamin, T.B., Bona, J.L., and Mahoney, J.J., Model equations for long waves in nonlinear dispersive systems, *Phil. Trans. Roy. Soc. London A* **272** (1972), 47–78.

[**8**] Boussinesq, J., Théorie des ondes et des remous qui se propagent le long d'un canal rectangulaire horizontal, en communiquant au liquide contenu dans ce canal des vitesses sensiblement pareilles de la surface au fond, *J. Math. Pures Appl.* **17** (2) (1872), 55–108.

[9] Boussinesq, J., Essai sur la théorie des eaux courants, *Mém. Acad. Sci. Inst. Nat. France* **23** (1) (1877), 1–680.

[10] Boyd, J.P., Weakly non-local solitons for capillary–gravity waves: fifth-degree Korteweg–deVries equation, *Physica D* **48** (1991), 129–146.

[11] Camassa, R., and Holm, D.D., An integrable shallow water equation with peaked solitons, *Phys. Rev. Lett.* **71** (1993), 1661–1664.

[12] Champneys, A.R., and Toland, J.F., Bifurcation of a plethora of multi-modal homoclinic orbits for autonomous Hamiltonian systems, *Nonlinearity* **6** (1993), 665–721.

[13] Eckhaus, W., On water waves at Froude number slightly higher than one and Bond number less than $\frac{1}{3}$, *Z. Angew. Math. Phys.* **43** (1992), 254–269.

[14] Eckhaus, W., Singular perturbations of homoclinic orbits in $\mathbb{R}^4$, *SIAM J. Math. Anal.* **23** (1992), 1269–1290.

[15] Gardner, C.S., Greene, J.M., Kruskal, M.D., and Miura, R.M., Method for solving the Korteweg–deVries equation, *Phys. Rev. Lett.* **19** (1967), 1095–1097.

[16] Grimshaw, R., Malomed, B., and Benilov, E., Solitary waves with damped oscillatory tails: an analysis of the fifth-order Korteweg–deVries equation, *Physica D* **77** (1994), 473–489.

[17] Hammersley, J.M., and Mazzarino, G., Computational aspects of some autonomous differential equations, *Proc. Roy. Soc. Lond. A* **424** (1989), 19–37.

[18] Hunter, J.K., and Scheurle, J., Existence of perturbed solitary wave solutions to a model equation for water waves, *Physica D* **32** (1988), 253–268.

[19] Hyman, J.M., and Rosenau, P., Pulsating multiplet solutions of quintic wave equations, preprint, Los Alamos National Labs, 1998.

[20] Il'ichev, A.T., Existence of a family of soliton-like solutions for the Kawahara equation, *Math. Notes* **52** (1992), 662–668.

[21] Il'ichev, A.T., and Marchenko, V.A., Propagation of long nonlinear waves in a ponderable fluid beneath an ice sheet, *Fluid Dyn.* **24** (1989), 73–79.

[22] Il'ichev, A.T., and Semenov, A.Yu., Stability of solitary waves in dispersive media described by a fifth-order evolution equation, *Theor. Comput. Fluid Dyn.* **3** (1992), 307–326.

[23] Ince, E.L., *Ordinary Differential Equations*, Dover, New York, 1956.

[24] Kakutani, T., and Ono, H., Weak non-linear hydromagnetic waves in a cold collisionless plasma, *J. Phys. Soc. Japan* **26** (1969), 1305–1318.

[25] Kawahara, T., Oscillatory waves in dispersive media, *J. Phys. Soc. Japan* **33** (1972), 260–264.

[26] Kichenassamy, S., Existence of solitary waves for water-wave models, *Nonlinearity* **10** (1997), 133–151.

[27] Kichenassamy, S., and Olver, P.J., Existence and non–existence of solitary wave solutions to higher order model evolution equations, *SIAM J. Math. Anal.* **23** (1992), 1141–1166.

[28] Li, Y.A., *Uniqueness and Analyticity of Solitary Wave Solutions*, Ph.D. Thesis, Penn State University, 1995.

[**29**] Malomed, B., and Vanden–Broeck, J.–M., Solitary wave interactions for the fifth-order KdV equation, *Contemp. Math.* **200** (1996), 133–144.

[**30**] Marchenko, V.A., Long waves in shallow liquid under ice cover, *J. Appl. Math. Mech.* **52** (1988), 180–183.

[**31**] Pomeau, Y., Ramani, A., and Grammaticos, B., Structural stability of the Korteweg–deVries solitons under a singular perturbation, *Physica D* **31** (1988), 127–134.

[**32**] Press, W.H., Teukolsky, S.A., Vetterling, W.T., and Flannery, B.P., *Numerical Recipes in C*: *The Art of Scientific Computing*, 2nd ed., Cambridge University Press, Cambridge, 1995.

[**33**] Rosenau, P., On nonanalytic waves formed by a nonlinear dispersion, *Phys. Lett. A* **230** (1997), 305–318.

[**34**] Sander, J., and Hutter, K., On the development of the theory of the solitary wave. A historical essay, *Acta Mech.* **86** (1991), 111–152.

[**35**] Scott Russell, J., On waves, *in*: *Report of the 14*th *Meeting*, British Assoc. Adv. Sci., 1845, pp. 311–390.

[**36**] Titchmarsh, E. C., *Theory of Functions*, Oxford University Press, London, 1968.

[**37**] Yamamoto, Y., and Takizawa, É.I., On a solution of nonlinear time-evolution equation of fifth order, *J. Phys. Soc. Japan* **50** (1981), 1421–1422.

[**38**] Zabusky, N.J., and Kruskal, M.D., Interaction of "solitons" in a collisionless plasma and the recurrence of initial states, *Phys. Rev. Lett.* **15** (1965), 240–243.
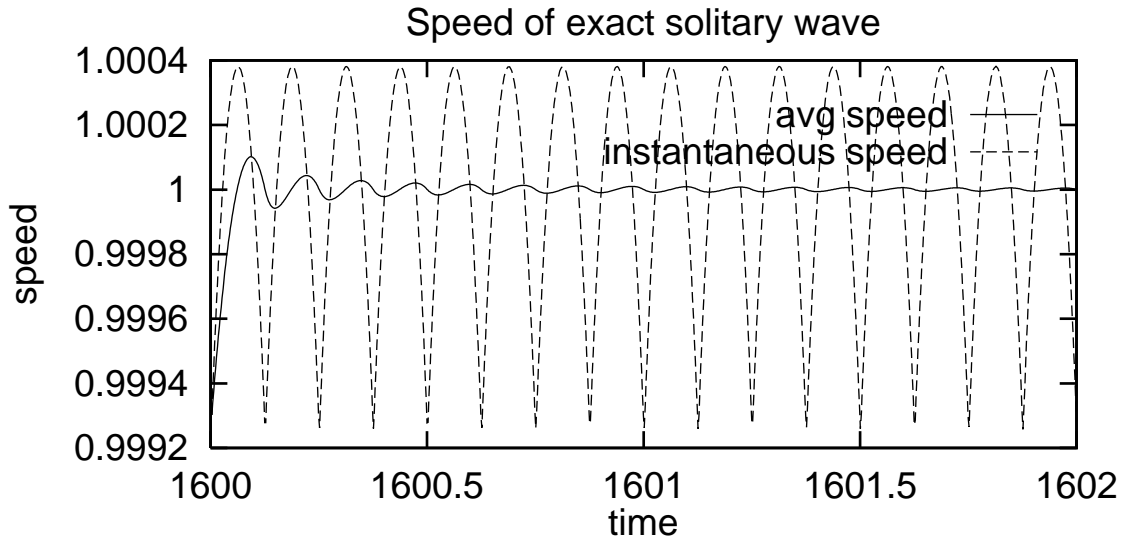
Figure 1.   Numerical speed of exact solitary wave solution
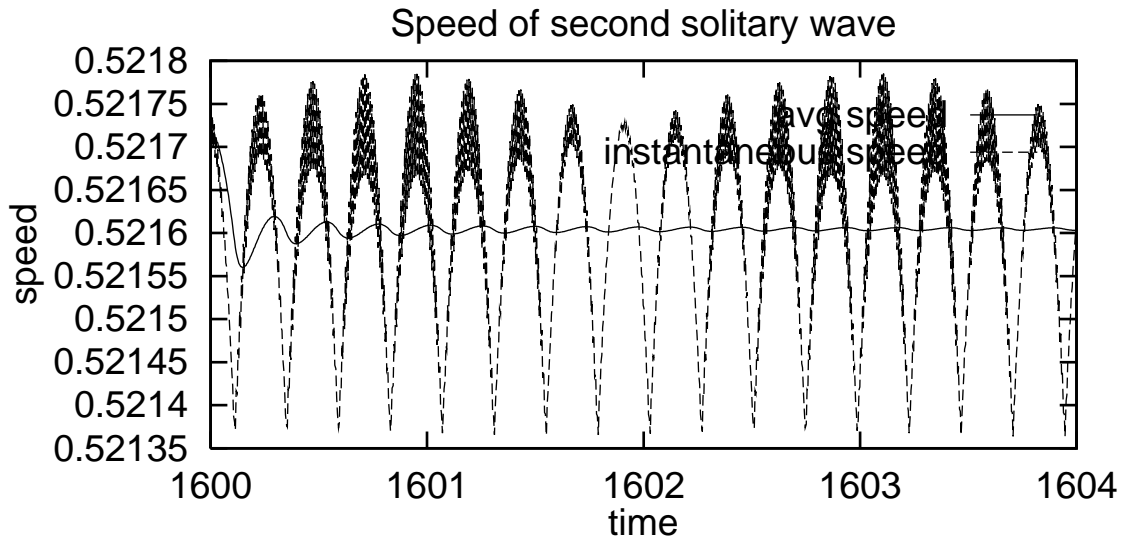
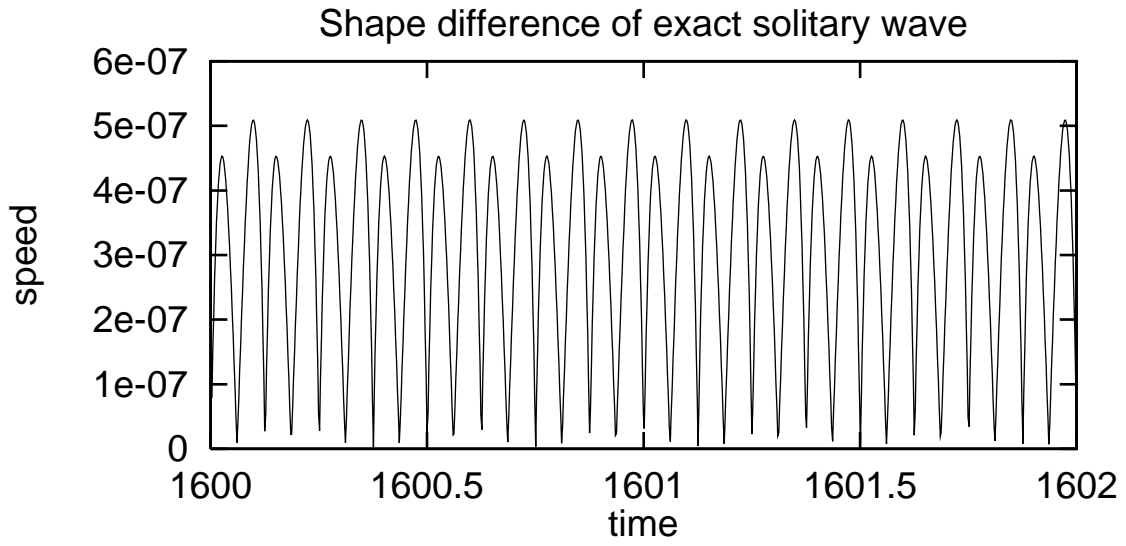Figure 2.   Numerical speed of second solitary wave solution
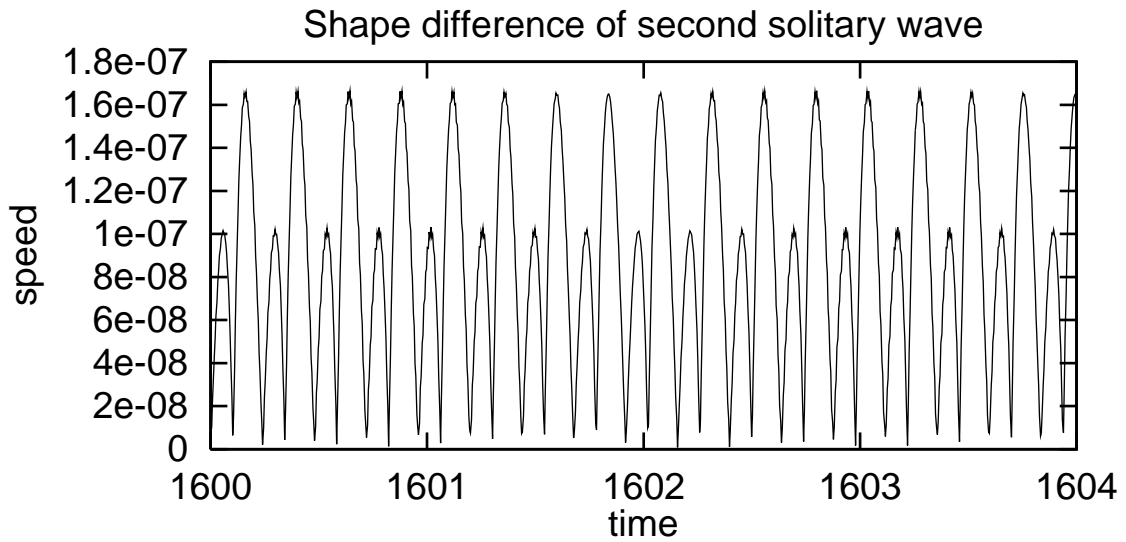
Figure 3.   Shape error of exact solitary wave solution

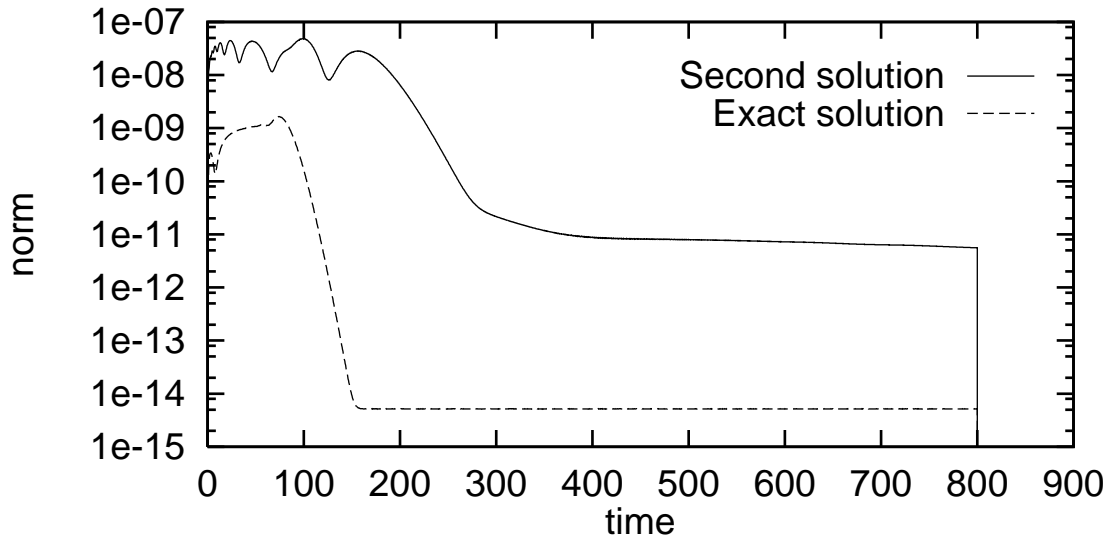

Figure 4.   Shape error of second solitary wave solution

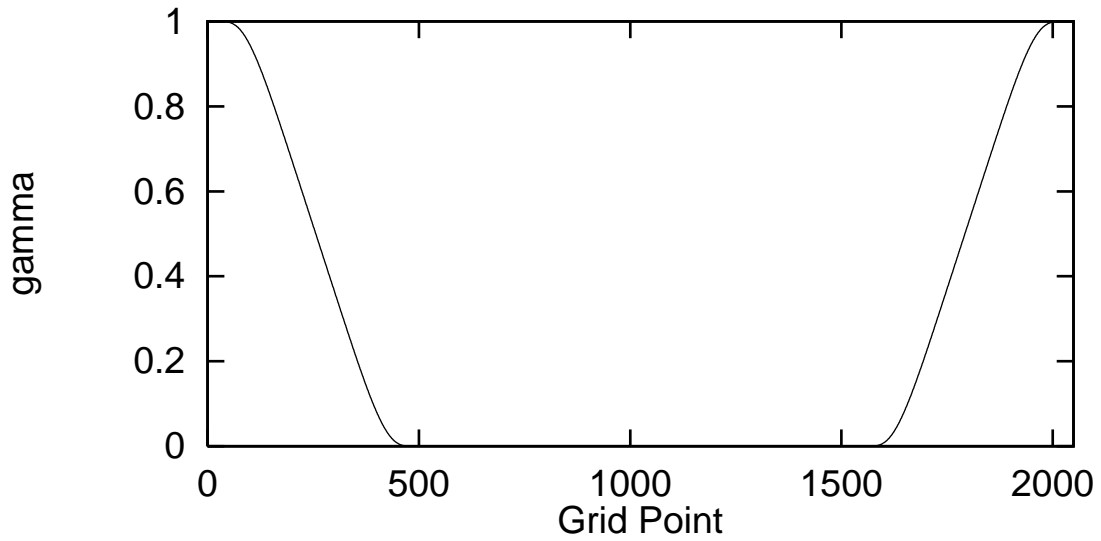Figure 5.   L^2 norm of damping effect
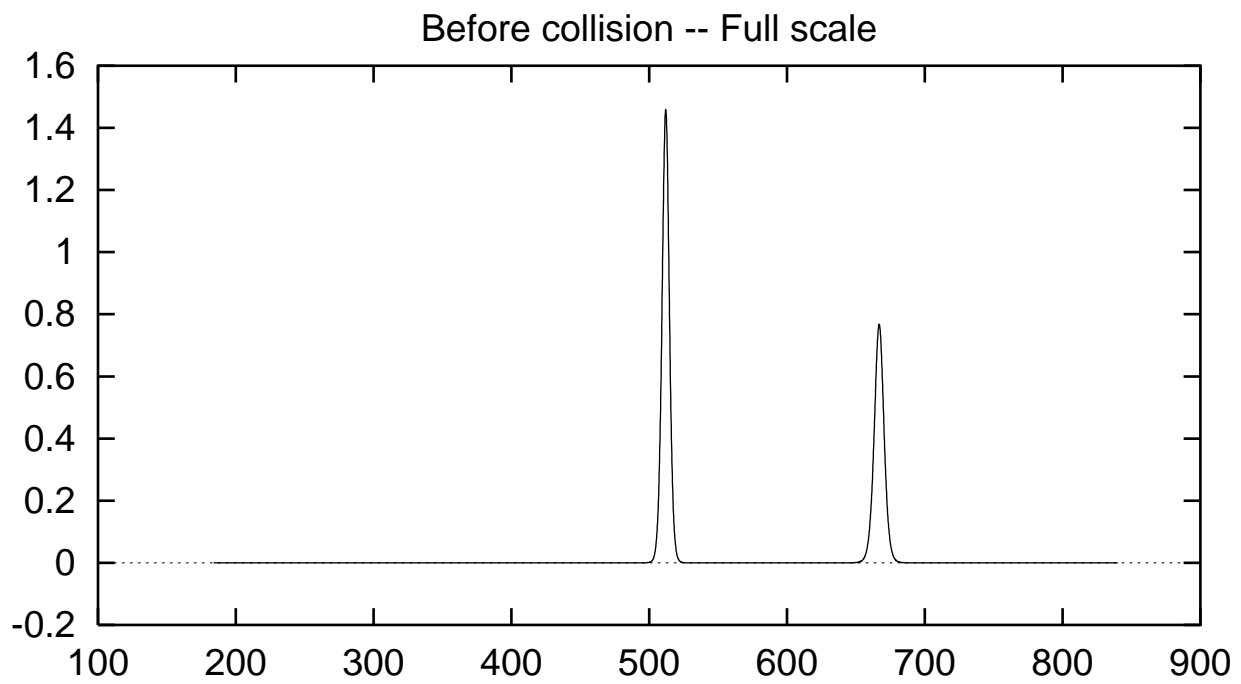

Figure 6.   Damping coefficient distribution

Figure 7.   Solution before collision (full scale)

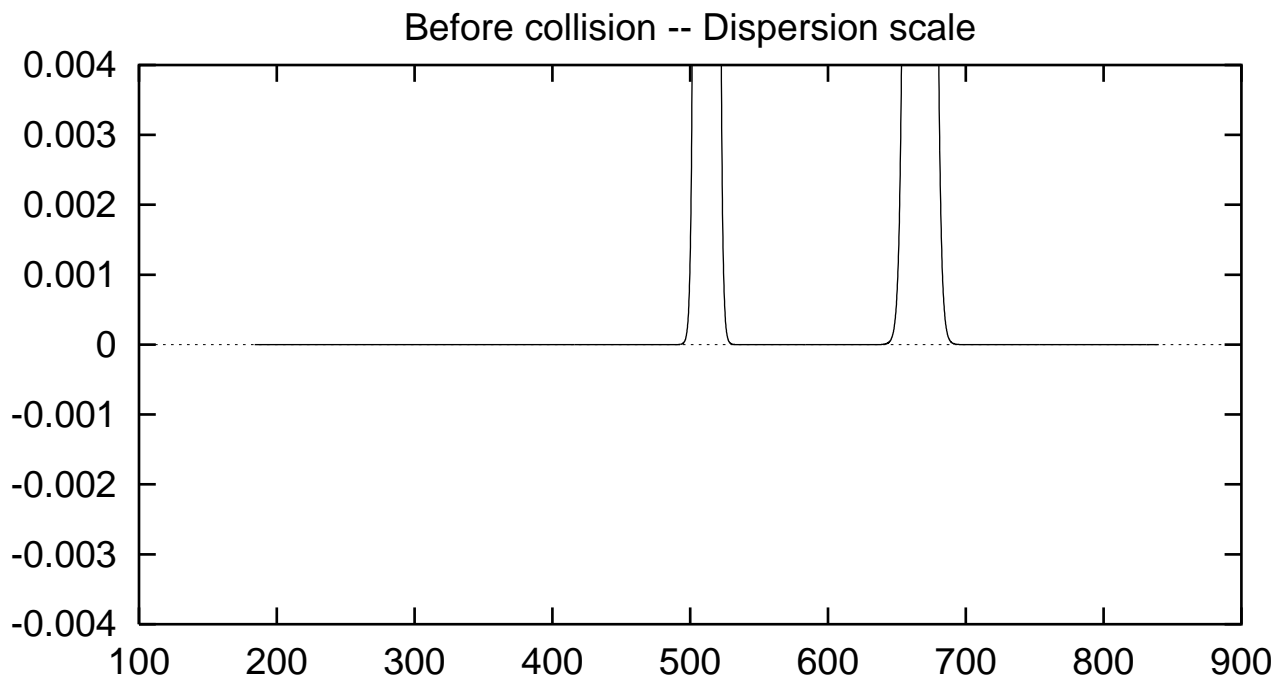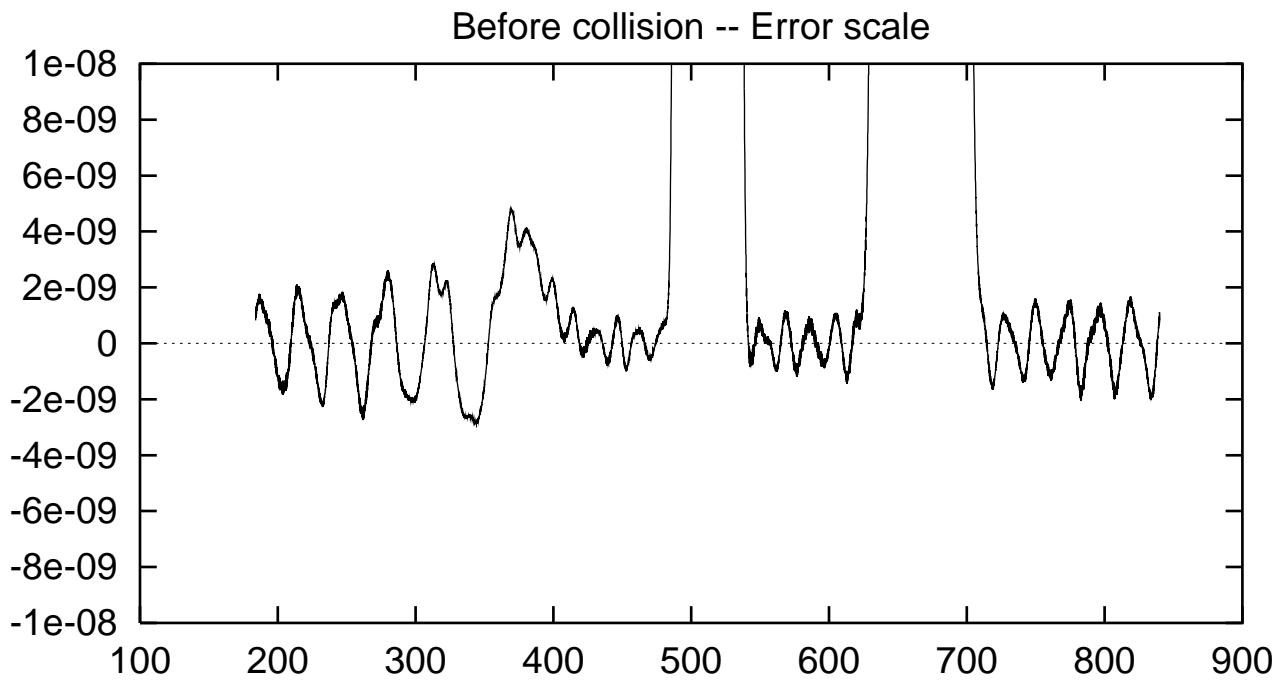Figure 8.   Solution before collision (dispersion scale)

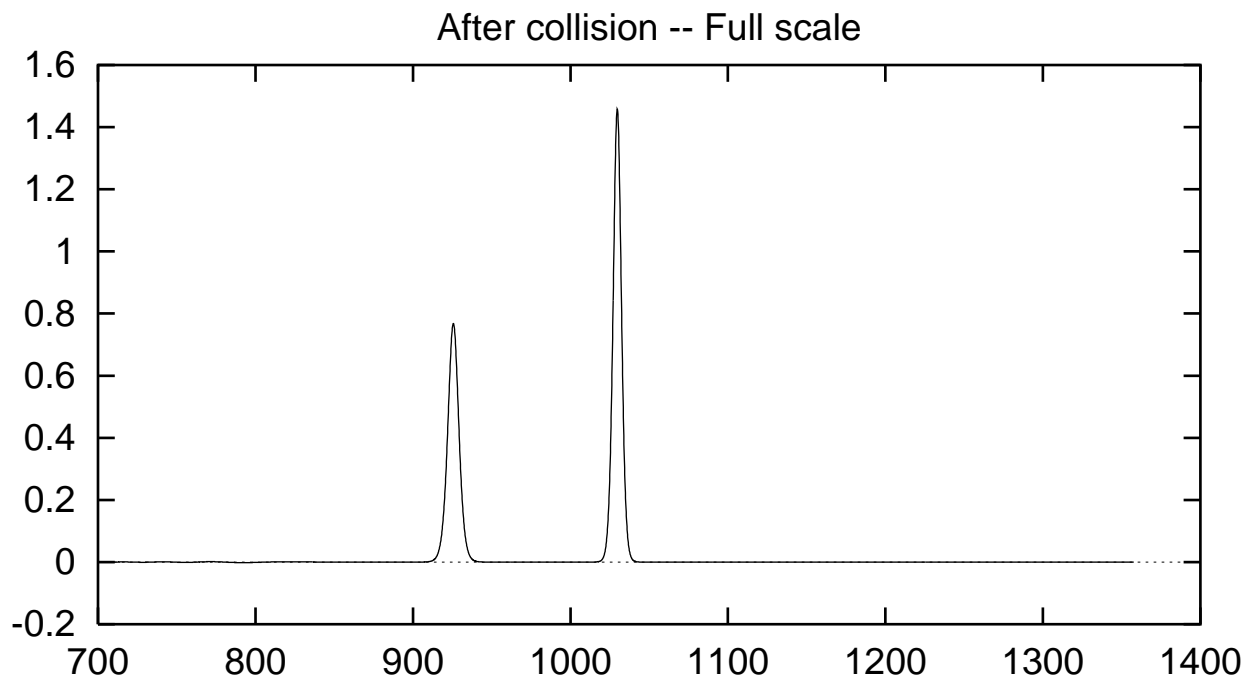Figure 9. Solution before collision (error scale)
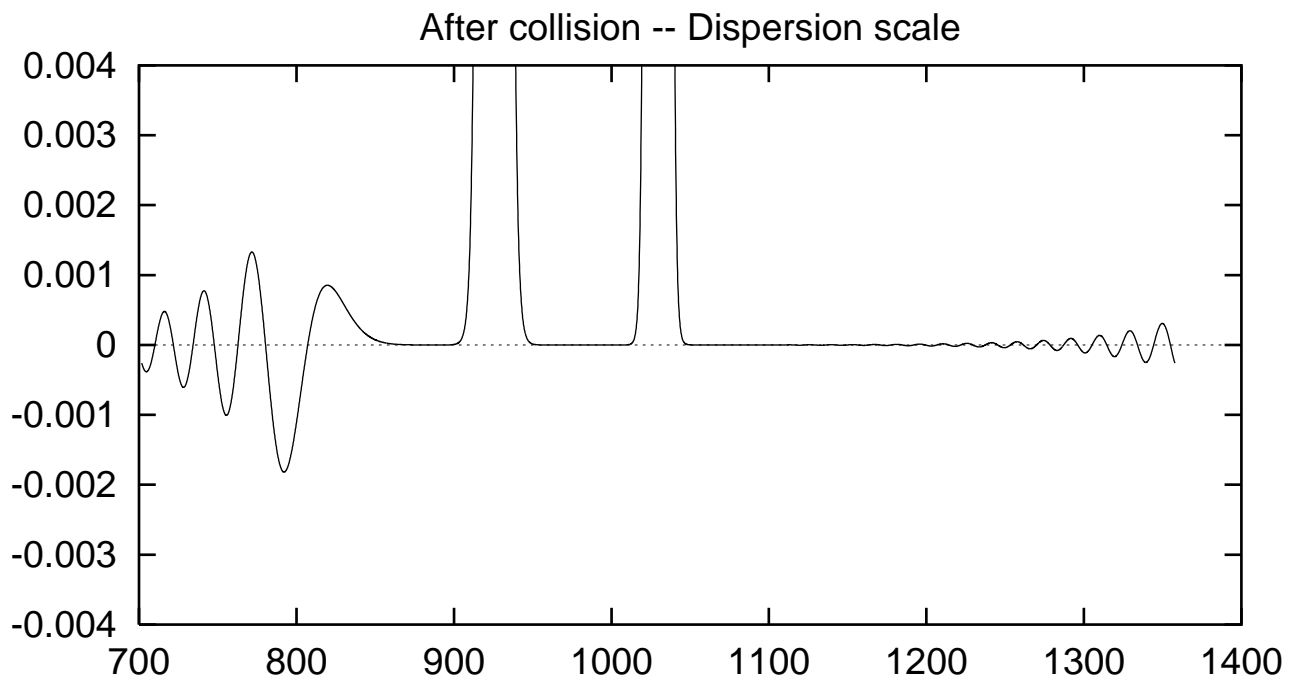

Figure 10. Solution after collision (full scale)

Figure 11.   Solution after collision (dispersion scale)